Available online at www.sciencedirect.com
SCIENCE DIRECT®

Trans. Nonferrous Met. Soc. China 18(2008) 804−808

Transactions of Nonferrous Metals Society of China

www.csu.edu.cn/ysxb/

Microstructure and properties of 7A52 Al alloy welded joint

HUANG Ji-wu(黄继武)[1, 2], YIN Zhi-min(尹志民)[1], LEI Xue-feng(雷学锋)[1, 3]

1. School of Materials Science and Engineering, Central South University, Changsha 410083, China;
2. Key Laboratory of Nonferrous Metal Materials Science and Engineering, Ministry of Education, Central South University, Changsha 410083, China;
3. Aerospace Research Institute of Materials and Processing Technology, Beijing 100076, China

Received 7 September 2007; accepted 15 February 2008

Abstract: 7A52 Al alloy plate aged at 105 ℃ for 8 h and then at 130 ℃ for 24 h was welded by means of TIG using Al-6.3Mg-0.35Sc-0.1Zr-0.1Cr solder wire. Mechanical properties and microstructures of welded joint were studied. There are two obviously soft areas in the welded joint, welding seam and over-aging zone. The mechanical properties of welded joint are that σ_b is 358 MPa, $\sigma_{0.2}$ is 238 MPa and δ_5 is 6.6%. 75.6% of welding coefficient can be achieved. The addition of scandium leads to very significant grain refinement in the fusion zone, which results in a reduction in solidification cracking tendency. The solidification cracking isn’t observed.

Key words: microalloying; Al alloy; welded joint; microstructure; mechanical properties

1 Introduction

Al-Zn-Mg alloys are hard to over-age during aging and insensitive to quench rate, which is an important issue for Al-Zn-Mg alloys in terms of welding[1]. 7A52 alloy is a medium-strength alloy among the Al-Zn-Mg systems and contains about 4.6% Zn and 2.5% Mg, which is increasingly used in light-mass structural applications, particularly in aircraft industry and armor plate structures[2−4]. In all cases, welding is the primary joining method. The final properties of the welded joint are attributed to the welding procedures, welding methods and solder wire. Many welding methods of 7A52 aluminum alloy have been reported[5−7]. These methods include metal inert gas arc welding (MIG), argon tungsten-arc welding (TIG) and friction stir welding (FSW), etc. For welded joint, the properties of weld seam are mainly determined by the chemical composition of wires[8−10]. In order to improve the mechanical properties of welded joint of Al-Zn-Mg alloys, a solder wire with proper composition should be selected.

In this work, the Al-6.3Mg-0.35Sc-0.1Zr-0.1Cr solder wire and TIG welding technique were selected to join the 5 mm-thick 7A52 aluminum alloy plates aged at 105 ℃ for 8 h and then at 130 ℃ for 24 h. The microstructures and mechanical properties in different welding zones were measured. The strengthening mechanism of different welding zones was studied.

2 Experimental

2.1 Materials and welding

Semi-continuous cast ingots of 7A52 alloy were supplied by Northeast Light Alloy Ltd. Co., China. The nominal compositions of the alloy are given in Table 1. The tested alloy was homogenized at 460 ℃ for 24 h and then hot-rolled at 420 ℃. The hot-rolled sheet was solution treated at 450 ℃ for 2 h and 470 ℃ for 1 h. Finally, it was aged at 105 ℃ for 8 h and at 130 ℃ for 24 h.

The nominal compositions of solder wire are given in Table 2.

Table 1 Chemical compositions of alloys(mass fraction ,%)

Zn	Mg	Mn	Cr	Cu	Fe	Si	Al
4.6	2.58	0.35	0.2 0	0.086	<0.15	<0.10	Bal.

Foundation item: Project(2005CB623705) supported by the National Basic Research Program of China
Corresponding author: HUANG Ji-wu; Tel: +86-731-8836426; E-mail huangjw@mail.csu.edu.cn

Table 2 Nominal compositions of solder wire(mass fraction,%)

Mg	Mn	Cr	Ti	Sc+Zr	Be	Si	Fe	Al
4.5−5.5	0.05−0.20	0.05−0.20	0.06−0.20	0.5−0.6	0.0008	≤0.15	≤0.15	Bal.

Solder wires have been developed by YIN el al[11]. The welding method was argon tungsten-arc welding (TIG). The welding parameters are given in Table 3.

Table 3 Welding parameters

Welding parameter	Value
Weldment thickness/mm	5
Welding wire diameter/mm	4
Injecting nozzle diameter/mm	12
Welding current/A	120−140
Gas flux/$(L\cdot min^{-1})$	10−14
Tungsten electrode diameter/mm	3

2.2 Properties and microstructure measurement

Tensile mechanical properties (σ_b, $\sigma_{0.2}$, δ_5) were tested on Instron 8032. The specimen size was 130 mm ×20 mm×5 mm. Hardness measurement was carried out at MHV2000SC micro hardness tester. X-ray diffraction patterns were measured on Rigaku D/Max 2500 diffractometer, and the diffraction conditions were 40 kV, 350 mA, step width 0.02˚, count time 2 s. Optical microscope(OM) observation was conducted on POLYVAR METHMV-2. TEM observation was conducted on FEI Tecnai G^{2}20, and operation voltage was 200 kV.

3 Results

3.1 Hardness distribution of welded joint

The hardness distribution of welded joint of 7A52 aluminum alloy is shown in Fig.1.

From Fig.1, it can be seen that the distribution of the hardness was symmetric in the welded joint. Among the joint, the hardness of the welding seam was the lowest, and it was the next lowest as the zone was about 20 mm away from the welding center, and hardness peak of welded joint appeared in the zone about 10 mm away from the welding center. About 30 mm away from the welding center, the hardness approached that of the 7A52 aluminum alloy based materials.

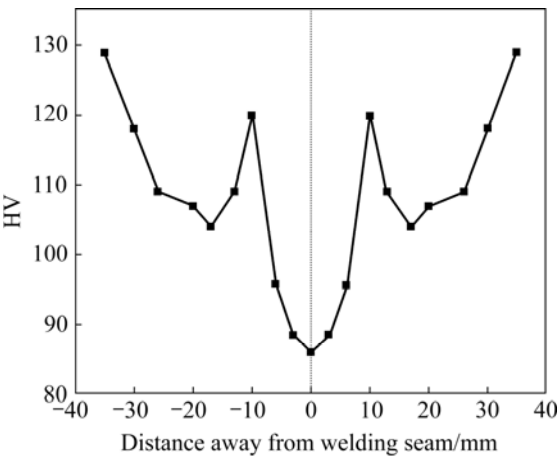

Fig.1 Hardness distribution of welded joint

3.2 Mechanical properties of welded joint

The tensile properties of solder wire and 7A52 aluminum alloy welded joint were measured and listed in Table 4.

Table 4 Tensile properties of solder wire, base material and welded joint

Specimen	σ_b/MPa	$\sigma_{0.2}$/MPa	δ_5/%
Wire	445	332	5.4
Base material	500	444	11.4
Welded joint	378	236	11.0

It can be seen from Table 4 that, the tensile properties of 7A52 aluminum alloy base materials were that σ_b was 500 MPa, $\sigma_{0.2}$ was 444 MPa and δ_5 was 10.4%. Those of welded joint were that σ_b was 378 MPa, $\sigma_{0.2}$ was 236 MPa and δ_5 was 11.4%. The tensile strength, yield strength and elongation of welded joint were lower than those of base materials. Welding coefficient approached 75.6%(coefficient of welding $K=\sigma_b^w/\sigma_b$, where σ_b^w is the tensile strength of welding interface, σ_b is the tensile strength of base materials).

3.3 Microstructure of welded joint

The microstructure of 7A52 aluminum alloy welded joint is shown in Fig.2.

In Fig.2, zone A was the welding seam, and its microstructure was composed of the equiaxial crystal

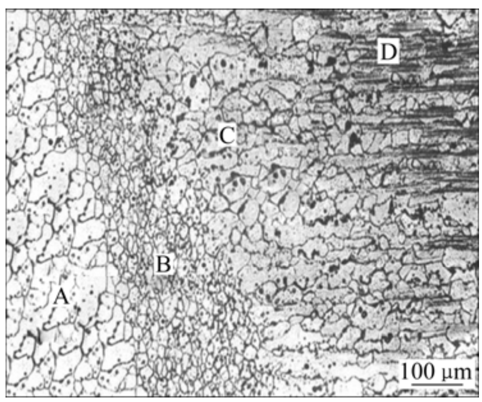

Fig.2 Microstructure of welded joint (A Welding seam; B Semi-melted zone; C Quenching zone; D Soften zone)

as-cast. The particle size was less than 40 μm. Zone B was the semi-molten zone, and its microstructure was the thin equiaxial crystal. Zone C was composed of the quenching zone. Its characteristic was the re-crystallization, and the re-crystallized grain was coarser than that of semi-molten zone. Zone D was the soften zone. It was near base material, and some microstructure was as-worked, but some re-crystallized grain was coarsened evidently.

3.4 X-ray diffraction of welding joint

The X-ray diffraction patterns of specimens which deviated different distances from the welding seam are shown in Fig.3.

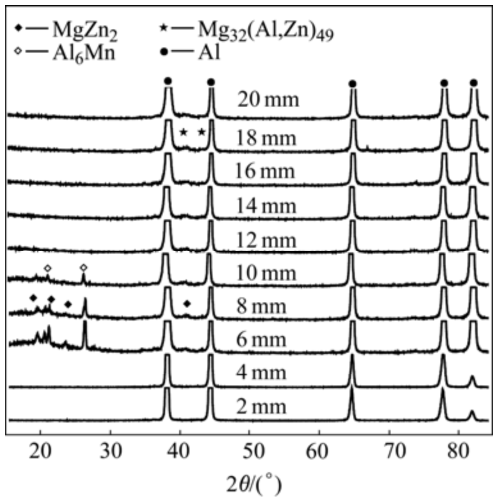

Fig.3 XRD patterns of specimens

From Fig.3, we can see that the structures were different with the different distances deviated from the welding seam. The XRD pattern of welding seam was displayed at the bottom of Fig.3, and its structure was composed of aluminum matrix only. The preferred orientation was in not detected by XRD patterns. Its structure was the as-cast state. The obvious precipitation diffraction peaks were found on the patterns of specimens deviated 6−10 mm from the welding seam. These precipitations were the $MgZn_2$ and Al_6Mn. The peaks of Al_6Mn were tall and narrow, and the peaks of $MgZn_2$ were broadened, i.e. the grain size of $MgZn_2$ was fine. The grain size of $MgZn_2$ was about 10 nm according to Scherrer formula $\beta=k\lambda/D \cos\theta$, and the precipitates $MgZn_2$ were mainly η' phase[4−12]. On the patterns of those specimens, which deviated further than 12 mm from the welding seam, the diffraction peak intensities of $MgZn_2$ decreased obviously. Only their cardinal diffraction peaks at the position of diffraction angle (2θ) about 42° could be found.

3.5 TEM observation of welded joint

The TEM images of welded joint of 7A52 aluminum alloy are shown in Fig.4.

The microstructure of welded seam was shown in Fig.4(a). Some nanometer particles can be seen in the view, and these particles were Al_3Zr, $Al_3(Sc, Zr)$, etc[9−10]. The microstructure of semi-molten zone was shown in Fig.4(b). In this zone, the nano-scale precipitations appeared in the grain, which were $MgZn_2$, Al_6Mn and Al_7Cr appeared in the grain boundary. Fig.4(c) shows the typical microstructure of the quenching zone. The primal precipitations re-dissolved partly into the Al matrix during welding and they transferred to supersaturated solid solution after cooling, and the nano-scale precipitations appeared again, which were attributed to the natural aging. The precipitated particles decreased obviously. The microstructure of softening zone was shown in Fig.4(d). Some re-crystallization structure can be found, and the precipitations coarsened obviously.

4 Discussion

4.1 Strengthening mechanism of different welding zones

The welded joint of the alloy was composed of welded seam and heat-affected zone.

The heat-affected zone consisted of semi-molten zone, quenching zone and softening zone.

For the semi-molten zone, very fine as-quenched equiaxed grains formed due to the high cooling rate and the scandium segregation (The grain size was about 5−10 μm) (see Fig.2). As the grains were deposited at room temperature, the nature ageing process occurred, the G.P. zone and $\eta'(MgZn_2)$ phases were precipitated from the as-quenched equiaxed grains (see Fig.3). The increase of strength was due to the extensive grain refinement and the nano-scale precipitations $\eta'(MgZn_2)$. The refinement of the solidification structure led to a reduction in solidification cracking tendency in this zone.

For the quenched zone, the welding temperature was higher than the solution temperature of the alloy. The primitive precipitation re-dissolved into the aluminum matrix, the microstructures were composed of re-crystallized as-quenched equiaxed grains, and the grain size became coarsening. During the grain was deposited at room temperature, the natural ageing process occurred, and this led to increase of the strength.

During the natural ageing treatment, the G.P. zone and η' phases precipitated[12]. These particles were in nano-scale which distributed homogeneously in the aluminum matrix. On the X-ray diffraction patterns, their diffraction peaks were broader than those of other phases (Fig.3). In addition, the main peaks of precipitation in zone deviated 6−10 mm from the welding seam appeared at about 19.8° (2θ); but in the base metal zones, the main

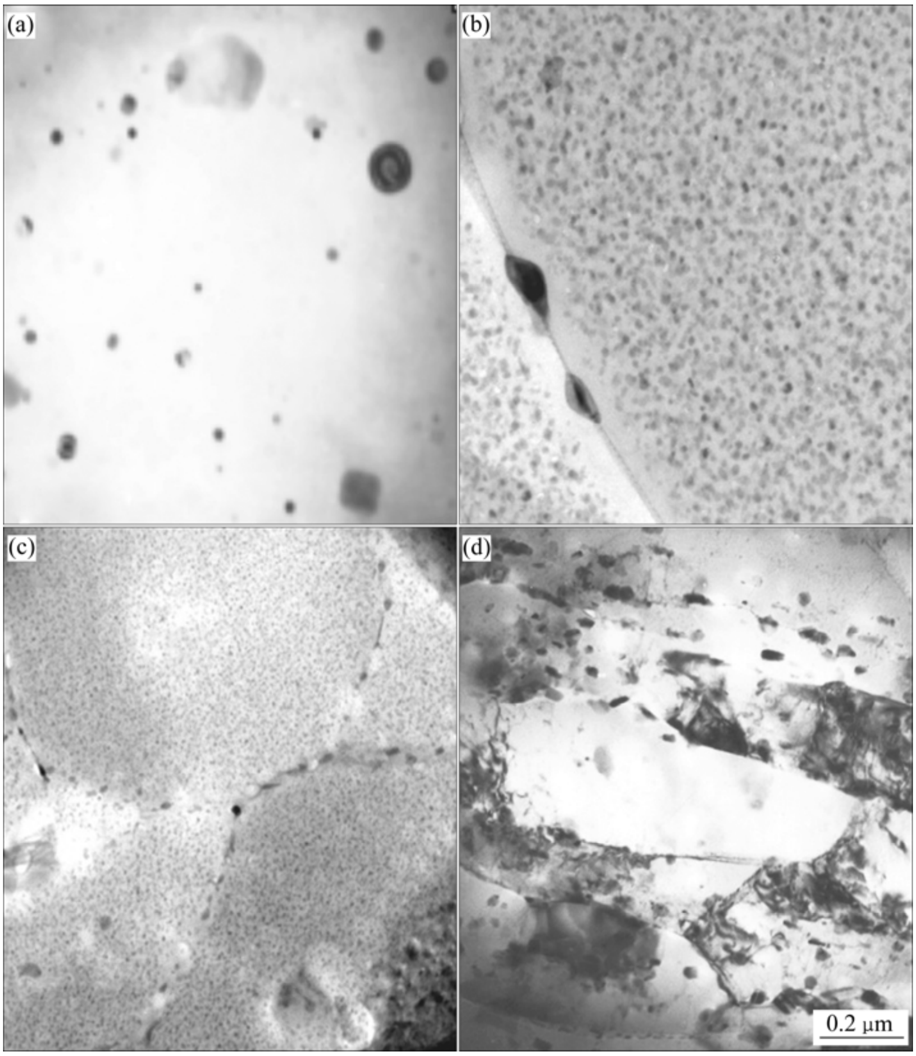

Fig.4 TEM images of weld joint: (a) Welding seam; (b) Semi-molten zone; (c) Quenching zone; (d) Softening zone

peaks of the precipitation appeared at about 42° (2θ). These small η' phases formed by the natural ageing treatment were of the disc-chip structure, and the phase of $\eta(MgZn_2)$ in the base material zones formed by the artificial aging was of the plank structures[12].

4.2 Effect of Sc addition on strength of welded joint

For the softening zone, the welded temperature was higher than the artificial aging temperature of the alloy. The η-precipitates became coarsening, and partly re-crystallization grains appeared. The strengthening of this zone decreased obviously. This zone was the weakest region in the heat-affected zone. The tensile strength of this zone can be expressed by

$$\sigma_b = \frac{2\sigma_s}{\sqrt{3}}(1+\frac{h}{4b})$$

where σ_s is the yield strength (MPa); b is the width of soften zone(mm); h is the thickness of base metal (mm).

The width of the over-aged zone was determined by the characteristic of base materials and weld process parameters. The lower the weld heat input (E) is, the narrower the over-aged zone is.

The properties of weld seam are mainly determined by the chemical composition of wires. Traditionally, refinement of most Al alloys relies on the inoculation of the alloy melts with Ti/TiB_2 master alloys[13]. However, this produces reasonable grain sizes at usual casting rates (100−150 μm), but it is very dependent on the melt contact time and no presence of poisoning elements, such as Fe and Si. However, debate still surrounds their exact mechanism of refinement, and there are many problems associated with their application. Literature suggests that Sc causes a far greater reduction in grain size that is possible with conventional refiners[14−16]. Additions of Zr combined with Sc restrict the formation of discontinuous transformation in the weld metal, which happens readily in binary Al-Zr alloys[9]. As welding of aluminum alloys is a fast cooling process, partially melted Al_3Sc particles within the welding seam could act as heterogeneous nuclei, resulting in grain refine. In this experiment, the Al-Mg welding wire with 0.5−0.6 Sc+Zr was used. The microstructures of scandium contained welded seam in regions near the weld centre are shown in Fig.2. Metallographic examination of fusion zones revealed that fine equiaxed grains formed in the fusion zone due to the addition of scandium. The refinement of the solidification structure led to a reduction in solidification cracking tendency, and solidification cracking wasn't observed. The strength of 7A52 aluminum alloy welded joint was σ_b=378 MPa, $\sigma_{0.2}$= 236 MPa. Welding coefficient of K reached 75.6%. The σ_b in welding seam with ER5356 was 356 MPa[8]. The tensile properties of welded joint were appreciably improved by adding scandium.

5 Conclusions

1) The mechanical properties of welded joint of 7A52 aluminum alloy by means of TIG welding using Al-6.3Mg-0.35Sc-0.1Zr-0.1Cr solder wire are σ_b=378 MPa, $\sigma_{0.2}$=236 MPa and δ_5=11%. Welding coefficient is 75.6%.

2) The addition of scandium leads to very significant grain refinement in the fusion zone, which leads to a reduction in solidification cracking tendency. The solidification cracking isn't observed.

3) There are two obviously soft areas in the welded joint, welding seam and over-aging zone. The decrease of the soft areas is attributed to the coarsening of the precipitation particles due to the welding heat cycle effect.

References

[1] FU Gao-feng, TIAN Fu-quan, WANG Hong. Studies on softening of heat-affected zone of pulsed-current GMA welded Al-Zn-Mg alloy[J]. Journal of Materials Processing Technology, 2006, 180: 216−220.

[2] ZHAO Jun-jun, WANG Wei-xin, CAI Zhi-hai, ZHANG Ping. Stress corrosion cracking susceptibility of 7A52 aluminum alloy [J]. Trans Nonferrous Met Soc China, 2006, 16: s1523−s1527.

[3] CHEN Kang-hua, HUANG Lan-ping, ZHENG Qiang, HU Hua-wen. Effect of high temperature pre-precipitation on stress corrosion cracking of 7A52 alloy[J]. Trans Nonferrous Met Soc China, 2005, 15(3): 442−445.

[4] HUANG Ji-wu, YIN Zhi-min, FANG Jia-fang, NIE Bo, WANG Tao. Aging characteristics of 7A52 Al-Zn-Mg alloy[J]. Materials Science Forum, 2007, 546/549: 867−870.

[5] YU Jin, WANG Ke-hong, XU Yue-lan, LIU Yong. Microstructure and properties of 7A52 aluminum alloy welding joint by twin wire welding[J]. Transactions of the China Welding Institution, 2005, 26(10): 87−90. (in Chinese)

[6] ZHOU Peng-zhan, ZHONG Jue, HE Di-qiu. Friction-stir welding on thick plate of 7A52 aluminum alloy[J]. The Chinese Journal of Nonferrous Metals, 2006, 16(6): 964−969. (in Chinese)

[7] LIU Ling-xia, CHENG Jian-gou, LU Fei. Research on fatigue behavior of welded 7A52 Al components[J]. Ordnance Material Science and Engineering, 2005, 28(5): 37−40. (in Chinese)

[8] WANG Sheng, LI Zhou, YIN Zhi-min, ZHOU Gu-xin, CEN Jian-gou. Microstructures and properties of welded joint of 7A52 alloy welded by the solder wire containing Sc and Zr[J]. Ordnance Material Science and Engineering, 2005, 28(03): 26−29. (in Chinese)

[9] NORMAN A F, HYDE K, COSTELLO F, THOMPSON S, BIRLEY S, PRANGNELL P B. Examination of the effect of Sc on 2000 and 7000 series aluminum alloy castings: For improvements in fusion welding[J]. Mater Sci and Eng A, 2003, 354: 188−198.

[10] SELVI D, ARCHIBALD A S, RAVI D K, MURTY B S, PRASAD R K. Effect of scandium additions on microstructure and mechanical properties of Al-Zn-Mg alloy welds[J]. Mater Sci Eng A, 2007, 467(15): 132−138.

[11] CHEN Su-li, JIANG Feng, YLN Zhi-min, LEI Xue-feng, NIE Bo. Microstructure and properties of Al-Mg-Sc alloy weld joints filled with Al-Mg-Zr-Sc weld wires[J]. The Chinese Journal of Nonferrous Metals, 2006, 16(5): 835-840. (in Chinese)

[12] MA T, OUDEN G D. Softening behavior of Al-Zn-Mg alloys due to welding[J]. Mater Sci Eng A, 1999, 266: 198–204.

[13] JANAKI R G D, MITRA T K, SHANKAR V, SUNDARESAN S. Microstructural refinement through inoculation of type 7020 Al-Zn-Mg alloy welds and its effect on hot cracking and tensile properties[J]. Journal of Materials Processing Technology, 2003, 142: 174−181.

[14] IRVI B. Scandium places aluminum welding on a new plateau[J]. Welding Journal, 1997, 76: 53−57.

[15] DAVGDOV V G, ROSTOVA T D, ZAKHAROV V V, YU A F, YELAING V I. Scientific principles of making an alloying addition of scandium to aluminum alloys [J]. Mater Sci Eng A, 2000, 280: 30−36.

[16] NORMAN A F, PRANGNEKK P B, MCEWEN R S. The solidification behavior of dilute aluminum-scandium alloys[J]. Acta Mater, 1998, 46(16): 5715−5732.

(Edited by LI Xiang-qun)